Journal of General Virology (2010), **91**, 907–914 DOI 10.1099/vir.0.018044-0

DNA photolyases of *Chrysodeixis chalcites* nucleopolyhedrovirus are targeted to the nucleus and interact with chromosomes and mitotic spindle structures

Fang Xu,[1] Just M. Vlak,[1] André P. M. Eker[2] and Monique M. van Oers[1]

Correspondence
Monique M. van Oers
monique.vanoers@wur.nl

[1]Laboratory of Virology, Wageningen University, PO Box 629, 6700 AP Wageningen, The Netherlands

[2]MGC-CBG Department of Cell Biology and Genetics, Erasmus University Medical Centre, PO Box 2040, 3000 CA Rotterdam, The Netherlands

Cyclobutane pyrimidine dimer (CPD) photolyases convert UV-induced CPDs in DNA into monomers using visible light as the energy source. Two *phr* genes encoding class II CPD photolyases PHR1 and PHR2 have been identified in *Chrysodeixis chalcites* nucleopolyhedrovirus (ChchNPV). Transient expression assays in insect cells showed that PHR1–EGFP fusion protein was localized in the nucleus. Early after transfection, PHR2–EGFP was distributed over the cytoplasm and nucleus but, over time, it became localized predominantly in the nucleus. Immunofluorescence analysis with anti-PHR2 antiserum showed that, early after transfection, non-fused PHR2 was already present mainly in the nucleus, suggesting that the fusion of PHR2 to EGFP hindered its nuclear import. Both PHR–EGFP fusion proteins strongly colocalized with chromosomes and spindle, aster and midbody structures during host-cell mitosis. When PHR2–EGFP-transfected cells were superinfected with *Autographa californica* multiple-nucleocapsid NPV (AcMNPV), the protein colocalized with virogenic stroma, the replication factories of baculovirus DNA. The collective data support the supposition that the PHR2 protein plays a role in baculovirus DNA repair.

Received 30 October 2009
Accepted 2 December 2009

INTRODUCTION

The genome of the baculovirus *Chrysodeixis chalcites* nucleopolyhedrovirus (ChchNPV) harbours two genes, Cc-*phr1* and Cc-*phr2*, that encode putative DNA-repair enzymes (van Oers *et al.*, 2004, 2005). Based on sequence comparisons, these genes encode DNA photolyases specific for cyclobutane pyrimidine dimers (CPDs), and it has been suggested that these genes are involved in viral DNA repair (van Oers *et al.*, 2005). CPDs as well as pyrimidine 6–4 pyrimidone photoproducts [(6–4)PP] are formed upon exposure of genomic DNA to UV light (UVB, 280–320 nm), but CPDs constitute the majority of UV-induced DNA lesions (Mitchell & Nairn, 1989; Rycyna & Alderfer, 1985; Setlow & Carrier, 1966). Dimeric pyrimidine photoproducts are cytotoxic, as they block transcription, may induce mutations and trigger apoptosis (Ljungman & Zhang, 1996; Nishigaki *et al.*, 1998; Chigançcas *et al.*, 2002).

Pyrimidine dimers can be repaired by several pathways, including photoreactivation (for a review, see Essen & Klar, 2006), nucleotide excision repair (NER) (reviewed by Schul *et al.*, 2002) and base excision repair (reviewed by Kimura *et al.*, 2004). Photoreactivation is the simplest and fastest DNA repair pathway, and uses only visible light as an energy source and involves a single enzyme, either a CPD or a (6–4)PP photolyase. Photoreactivation occurs in all groups of organisms, except placental mammals, which have to rely on the NER pathway to repair pyrimidine dimers (Yasui *et al.*, 1994).

CPD photolyases are monomeric proteins of 450–550 amino acids and carry a flavin adenine dinucleotide (FAD) molecule as a catalytic co-factor. Besides FAD, many CPD photolyases also contain a light-harvesting co-factor, which is either 5,10-methenyltetrahydrofolate (MTHF) or an 8-hydroxy-7,8-didemethyl-5-deazaflavin (8-HDF). The light-harvesting co-factor captures near-UV or blue light photons. The excitation energy is transferred to FAD and used to donate an electron to a CPD, leading to the conversion of the pyrimidine dimer into monomers (reviewed by Deisenhofer, 2000; Essen & Klar, 2006; Hearst, 1995; Sancar, 1994, 2003).

CPD photolyases have traditionally been categorized into two classes, I and II, based on comparison of their amino acid sequences. Phylogenetic analysis suggests that type I

A supplementary table is available with the online version of this paper.

and type II CPD photolyases have a common ancestor but diverged early in evolution (Yasui *et al.*, 1994). The two CPD photolyases encoded by the baculovirus ChchNPV share 45 % identity at the amino acid level and belong to class II (van Oers *et al.*, 2005; Xu *et al.*, 2008). Homologues of the ChchNPV *phr* genes have been found in *Trichoplusia ni* single-nucleocapsid NPV (TnSNPV) (Willis *et al.*, 2005) and *Spodoptera litura* granulovirus (SpliGV) (Wang *et al.*, 2008). ChchNPV and TnSNPV are closely related viruses that infect insects of the subfamily Plusiinae of the Noctuidae. Recent studies revealed that *phr* genes are conserved in plusiine-infecting group II NPVs (Xu *et al.*, 2008) of the genus *Alphabaculovirus* (Jehle *et al.*, 2006).

The activity of the ChchNPV PHR proteins has been examined in complementation assays in a DNA repair-deficient *Escherichia coli* strain, showing that Cc-*phr2* encodes an active CPD photolyase (van Oers *et al.*, 2008). In contrast, the photolyase deficiency in *E. coli* could not be rescued with Cc-*phr1*. Cc-PHR2 photolyase also repaired CPD dimers *in vitro* and spectral measurements demonstrated the presence of FAD. Reconstitution experiments suggested that Cc-PHR2 uses an 8-HDF as a second co-factor (van Oers *et al.*, 2008). To be able to repair DNA damage in a baculovirus genome, PHR proteins need to be targeted to the nucleus, as baculoviruses replicate and assemble in the nucleus of insect cells, and they should have the ability to bind DNA.

In the current study, the intercellular localization of the two ChchNPV PHR proteins was studied using enhanced green fluorescent protein (EGFP) fusion constructs transiently expressed in insect cells. The intracellular localization of the Cc-PHR–EGFP proteins was determined based on the distribution of the EGFP fluorescence signal. Moreover, the effect of baculovirus infection on the localization of the Cc-PHRs was investigated, as the presence of viral proteins and large amounts of viral DNA during infection might influence the targeting of these photolyases. The cellular distribution of Cc-PHR2 was also studied by immunofluorescence to support the observations with EGFP.

RESULTS

Localization of PHR1 in insect cells

To investigate the subcellular localization of ChchNPV photolyases in insect cells, expression plasmids were constructed to produce the PHR proteins fused to the N terminus of EGFP (Fig. 1a, b). A non-fused EGFP construct served as a control (Fig. 1c). After transfection into insect cells, the PHR1–EGFP fusion was localized predominantly in the nucleus from 28 h until 120 h post-transfection (p.t.) (Fig. 2a–d). Non-fused EGFP, on the other hand, was distributed homogeneously over the cytoplasm and the nucleus at all time points analysed, as shown for 96 h p.t. (Fig. 2e).

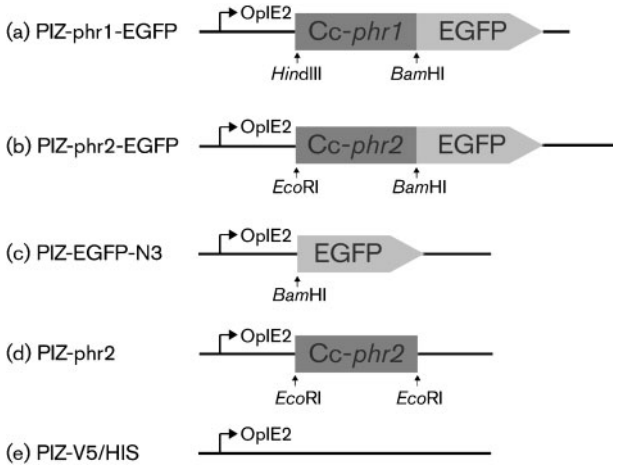

Fig. 1. Schematic diagrams of the various constructs used in the study. The ChchNPV *phr1* (a) and *phr2* (b) ORFs were fused to the N terminus of EGFP under control of the OpMNPV OpIE2 promoter. The non-fused EGFP (c) served as a control. The *phr2* ORF was cloned into the PIZ-V5/HIS vector for immunofluorescence assays (d), for which the vector (e) served as a control.

To determine whether baculovirus infection affected the subcellular localization of PHR1, cells were infected with *Autographa californica* multiple-nucleocapsid NPV (AcMNPV) at 24 h p.t. and examined for EGFP fluorescence during the course of infection. In the early phase of AcMNPV infection (4 h p.i.) (Fig. 2f, k), the PHR1–EGFP fusion protein showed a nuclear localization similar to that at 28 h p.t. without infection. At 24 h p.i., when virogenic stroma appeared in the centre of the nucleus of infected cells (Fig. 2g, l), the fluorescence was present uniformly in the cytoplasm as well as in the nucleus. At 48 and 72 h p.i., many viral occlusion bodies or polyhedra were seen in the nucleus of infected cells and fluorescence was seen in both the cytoplasm and nucleus (Fig. 2h–i, m–n). Strong fluorescence was not observed in virogenic stroma or in the viral occlusion bodies. The distribution of non-fused EGFP was not affected by AcMNPV infection until polyhedra were produced, when reduced nuclear EGFP fluorescence was observed (Fig. 2j, o).

Localization of PHR2 in insect cells

In a similar way, cells transfected with PIZ-phr2–EGFP were examined by confocal laser scanning microscopy at various time points after transfection (Fig. 3). Initially, the PHR2–EGFP fusion protein was found in the cytoplasm as well as in the nucleus (Fig. 3a, b). In the cytoplasm, an intense, ring-shaped fluorescence was seen along the nuclear membrane, especially at 28 h p.t. (Fig. 3a). Over time, the PHR2–EGFP protein accumulated in the nucleus. At 72 and 96 h p.t., the nucleus was marked by intense fluorescence, although some fluorescence still remained in

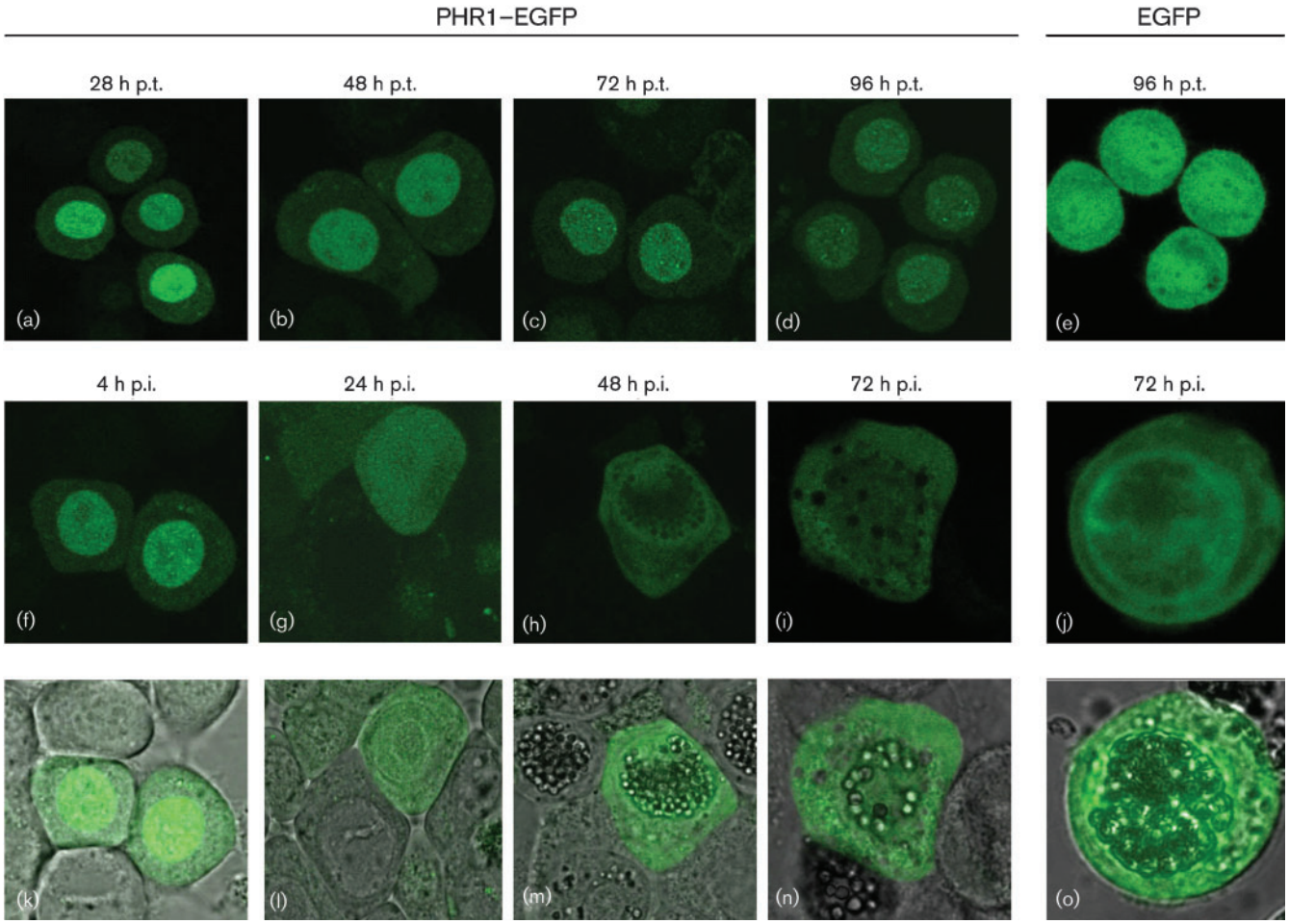

Fig. 2. Subcellular localization of the PHR1–EGFP fusion protein in transiently transfected *T. ni* High Five cells. (a–d) Time-course fluorescence micrographs of transiently expressed PHR1–EGFP. (f–i) Time-course fluorescence examination of PHR1–EGFP, following an AcMNPV infection at 24 h post-transfection (p.t.). (k–n) Overlay images of fluorescence (f–i) and phase-contrast micrographs. The localization of non-fused EGFP under the various conditions is shown on the right (e, j, o).

the cytoplasm (Fig. 3c, d). When cells were infected with AcMNPV following transfection, a substantial amount of PHR2–EGFP was detected in the nucleus of infected cells at 4 h p.i. (28 h p.t.) (Fig. 3e). At 24, 48 and 96 h p.i., some PHR2–EGFP fusion protein was still detected in the cytoplasm, but the majority was localized in a central area of the nucleus, colocalizing with virogenic stroma (Fig. 3f–h), in contrast to PHR1. Viral occlusion bodies or polyhedra did not show green fluorescence (Fig. 3k, l).

ChchNPV photolyases during mitosis

In the transient expression assays, both PHR1– and PHR2–EGFP fusion proteins associated clearly with chromosomes of *T. ni* High Five cells during mitosis. Complete mitotic cycles could be visualized by tracing the PHR2–EGFP protein in the cell (Fig. 4), as chromosome binding by the PHR2–EGFP fusion protein was readily evident in the prophase (Fig. 4a), prometaphase (Fig. 4b), metaphase (Fig. 4c) and anaphase (Fig. 4d). During cell division, the mitotic spindle and the aster structure were also visible by green fluorescence (Fig. 4c, d), but with much less intensity than the chromosomes. New nuclear membranes were indicated by ring-shaped fluorescence appearing at the telophase (Fig. 4f). The midbody, the remainder of the spindle, was also marked by green fluorescence (Fig. 4e, f). Chromosome binding by PHR1–EGFP was also observed during mitosis, but with relatively weak intensity compared with PHR2–EGFP, which may be explained by lower expression levels of *phr1–egfp* in the cells. Less PHR1–EGFP accumulation was observed in all confocal studies and was confirmed by Western blot analysis with anti-EGFP antiserum (data not shown).

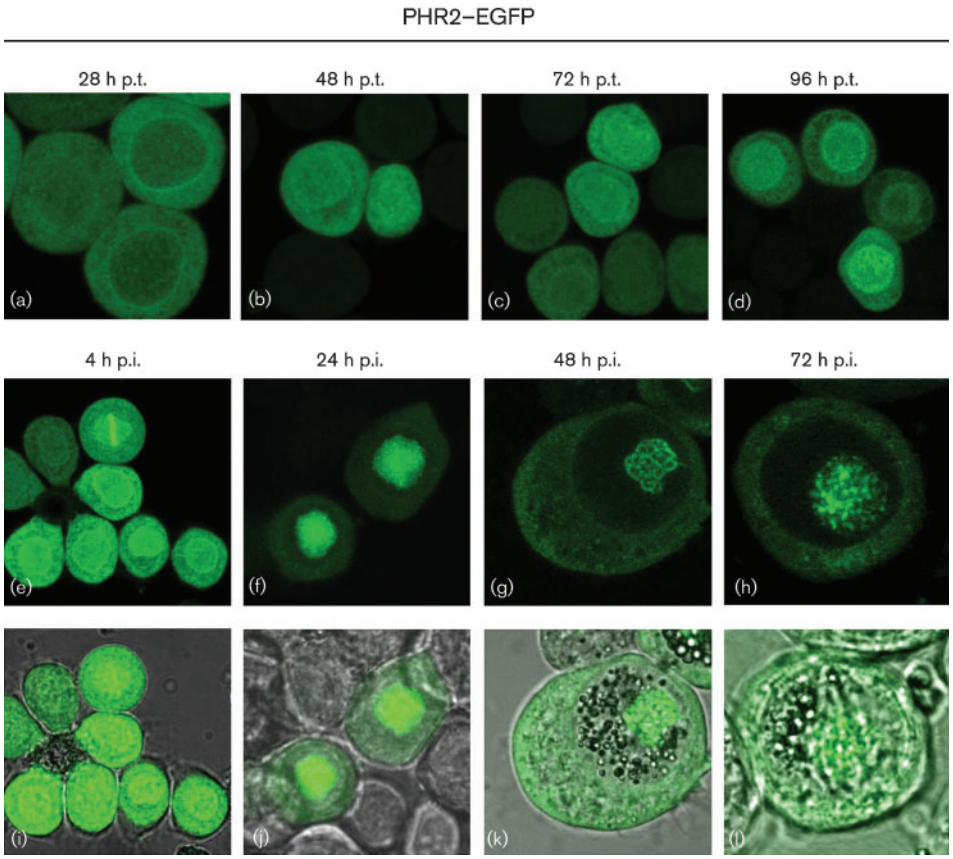

Fig. 3. Subcellular localization of PHR2–EGFP fusion proteins in transiently transfected *T. ni* High Five cells. (a–d) Time-course fluorescence micrographs of transiently expressed PHR2–EGFP. (e–h) Time-course fluorescence detection of PHR2–EGFP with AcMNPV infection at 24 h p.t. (i–l) Overlay of fluorescence (e–h) and phase-contrast micrographs. For non-fused EGFP alone, see Fig. 2.

Location of PHR protein in transfected cells using photolyase-specific antibodies

Expression of *phr2–egfp* and non-fused *phr2* in transfected *T. ni* High Five cells was analysed by Western blot analysis at 24 h p.t. using polyclonal PHR2 antiserum. This serum was raised by immunization of rabbits with purified recombinant PHR2 protein. The analysis of total extracts of cells transfected with PIZ-phr2 (Fig. 1d) revealed that the antibody recognized non-fused PHR2 as a 53 kDa protein, slightly different from the predicted value of 57.3 kDa, but with electrophoretic properties similar to those of recombinant PHR2 produced in bacteria (Fig. 5, lanes 1 and 2). The PHR2–EGFP fusion protein was detected as a single ~83 kDa protein (Fig. 5, lane 3), also slightly smaller than the predicted value of 85 kDa. These results verified that the anti-PHR2 antibody recognizes PHR2 in cell extracts. It also shows that PHR2–EGFP was present as a full-length fusion protein. Western blot analysis performed with anti-EGFP antibody confirmed the expression of full-length fusion products for both PHR1–EGFP and PHR2–EGFP (data not shown). The anti-PHR2 antiserum showed a weak cross-reactivity to a ~55 kDa cellular protein, as judged from its appearance in cells transfected with the empty vector, PIZ-V5/HIS (Fig. 5, lane 4).

Nuclear localization of PHR2 by immunofluorescence analysis

After testing the performance of the anti-PHR2 antibody by Western blot analysis of transfected cells, the localization of non-fused PHR2 in transfected cells was studied by immunofluorescence analysis. Rhodamine fluorescence revealed that the transiently expressed non-fused PHR2 protein was localized primarily in the nucleus and was already present there at 24 h p.t. (Fig. 6a). At this time point, the PHR2–EGFP fusion protein was detected with the antiserum in both the cytoplasm and the nucleus with a homogeneous distribution (Fig. 6d). The PHR2–EGFP localization was similar to that described above in the EGFP fluorescence studies (see also Fig. 3), as can be seen in a merged image of green and red fluorescence (Fig. 6e, f). Mock-transfected cells and cells transfected with PIZ-V5/HIS only showed a very weak rhodamine fluorescence, which should be regarded as background labelling (Fig. 6b, c).

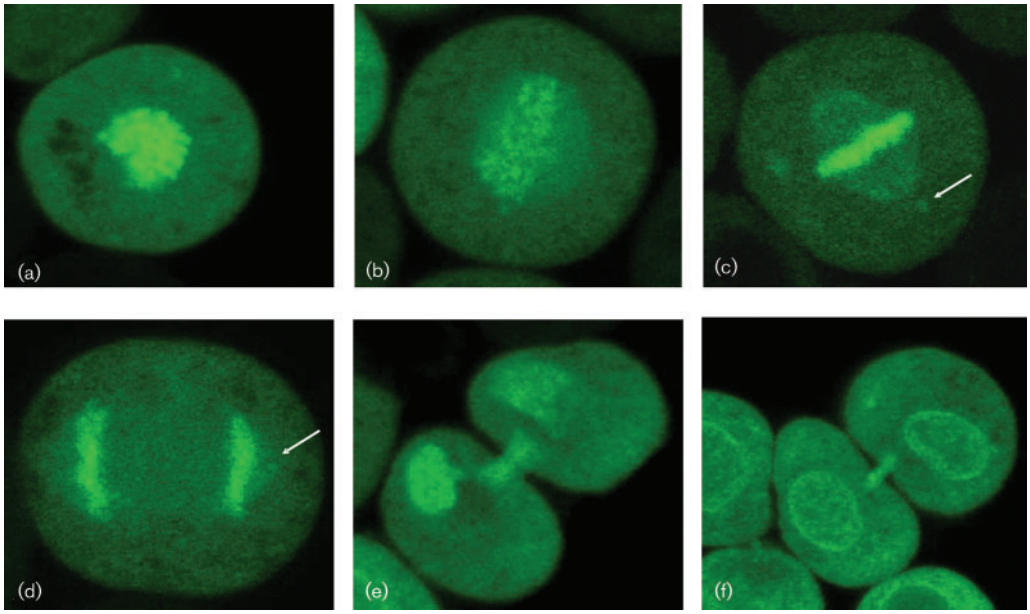

Fig. 4. Chromosome binding of PHR2. PHR2–EGFP-expressing cells were analysed at 24 h p.t. PHR2–EGFP is associated with chromosomes, spindle and aster structures during the various stages of mitosis (a–f). Aster structures are indicated by arrows. The remains of the polar spindles can be seen as midbody (e, f) towards the end of cell division.

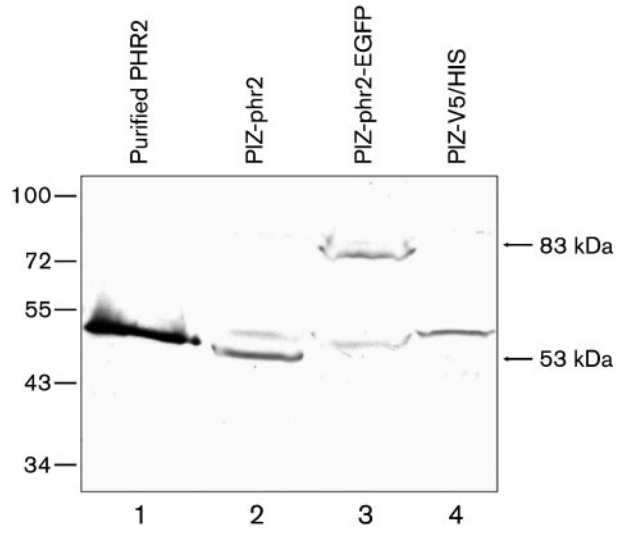

Fig. 5. Immunoblot analysis of PHR2 and PHR2–EGFP expression in transfected *T. ni* High Five cells using anti-Cc-PHR2 antibody. Purified recombinant PHR2 was used as a control (lane 1). *T. ni* High Five cells were transfected with PIZ-phr2 (lane 2), PIZ-phr2-EGFP (lane 3) or PIZ-V5/HIS (lane 4). Positions of molecular mass markers are indicated on the left in kDa. The observed molecular mass of PHR2 (53 kDa) and the PHR2–EGFP fusion protein (83 kDa) is indicated on the right.

DISCUSSION

Baculoviruses are used widely as biocontrol agents of insect pests. However, these viruses are very sensitive to and quickly inactivated by UV irradiation (Fritsch & Huber, 1985; Ignoffo & Garcia, 1992; Vail *et al.*, 1999). The inactivation rate of baculoviruses correlates well with the UV dose received (Sun *et al.*, 2004). A functional CPD photolyase may repair pyrimidine dimers and thereby increase the UV resistance of progeny virions and enhance their persistence in the environment. Therefore, an active photolyase would be an ecological benefit for a baculovirus, and ChchNPV seems to encode two such enzymes.

In this paper, the subcellular localization of Cc-PHR1 and Cc-PHR2 was examined in *T. ni* High Five cells using a transient expression system with EGFP as a reporter. PHR1–EGFP was localized predominantly in the nucleus, and the distribution pattern did not change over time. Compared with PHR1–EGFP, it took longer for the PHR2–EGFP fusion protein to localize completely to the nucleus (Figs 2 and 3). The expression level of *phr2–egfp* was much higher than that of *phr1–egfp*, as judged by the difference in intensity of the EGFP fluorescence in cells and confirmed by Western blot analysis. This may explain why not all of the PHR2–EGFP protein was imported into the nucleus within a short period of time. When cells were infected with virus, nuclear import was accelerated, leading to the hypothesis that PHR2–EGFP may require viral chaperones to enter the nucleus. However, when non-fused PHR2 was analysed by applying immunofluorescence methods, it was transported efficiently into the nucleus (Fig. 6), showing

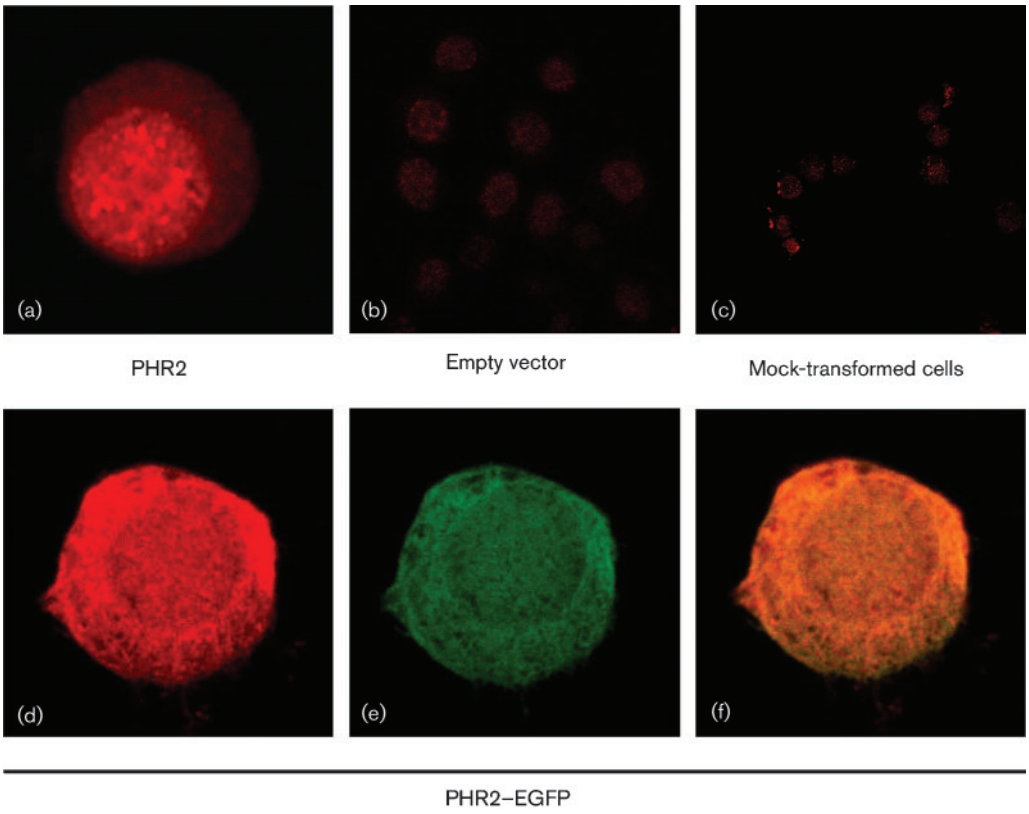

Fig. 6. Subcellular localization of PHR2 and PHR2–EGFP in transected *T. ni* High Five cells by immunofluorescence using anti-Cc-PHR2 serum. Rhodamine fluorescence signals the expression of PHR2 at 24 h p.t. (a), while no signal is observed in cells transfected with PIZ-V5/HIS (b) or mock-transfected cells (c). Rhodamine fluorescence of cells expressing PHR2–EGFP at 24 h p.t. (d) is compared with EGFP fluorescence (e), and the two images have been merged (f). Panels (b) and (c) were taken at low magnification to show that all cells lack fluorescence.

that the fusion of PHR2 to EGFP is responsible for the distribution of the fusion product over nucleus and cytoplasm.

In this study, the effect of virus infection on the localization of Cc-PHR proteins was analysed in order to simulate the more natural situation of virus infection. The idea behind this is that other viral proteins or the presence of large amounts of replicating viral DNA may affect the intracellular distribution of the PHR proteins. The choice was made to infect the transfected cells with the baculovirus AcMNPV, since a fully permissive cell line for ChchNPV is not available. Trials with ChchNPV infections in the semi-permissive *T. ni* High Five cells showed that, despite the limitations, PHR–EGFP fusion proteins were also routed to the nucleus in these cells (not shown).

In the presence of a virus infection, the PHR1–EGFP fusion product was found in the nucleus and in the cytoplasm with an approximately homogeneous distribution (Fig. 2). PHR2–EGFP localized primarily to a central region of the nucleus in the late phase of AcMNPV infection, which probably corresponds to the virogenic stroma. This is considered as a de novo product of baculovirus infection, in which viral DNA is replicated and progeny virions are assembled (Williams & Faulkner, 1997; Rohrmann, 2008). The enhanced nuclear import and association of PHR2 with virogenic stroma might be explained by the potential interaction between PHR2 and certain viral proteins or the capacity of PHR2 to bind newly synthesizing or synthesized viral DNA. In a previous study, we used oligonucleotides with thymine dimers and showed that the PHR2 protein was able to repair these dimers, which does imply a direct interaction with DNA (van Oers *et al.*, 2008). No fluorescence was found in polyhedra upon infection with AcMNPV (Fig. 3), which may indicate that PHR2 (as well as PHR1) is not incorporated in progeny virions, or at least not in large amounts. This is in line with the fact that we were unable to show the presence of PHR2 or PHR2–EGFP in polyhedra isolated from these cells by Western blotting (not shown). However, low levels of PHR proteins may not be detectable in this way, and the fluorescence data may be affected by absorption of light from the laser beam or the emitted fluorescence by the polyhedrin protein surrounding the virus particles.

PHR1 showed a different intranuclear distribution in infected cells from that of PHR2. A previous study showed

that PHR1 was not an active photolyase when tested in a bacterial system deficient in DNA repair (van Oers *et al.*, 2008). This may be explained by the fact that a conserved tryptophan, which may be involved in electron transfer (Aubert *et al.*, 2000), is absent in PHR1 (van Oers *et al.*, 2008). Whether PHR1 is an active photolyase in insect cells or baculovirus particles is not known, but a preference for virogenic stroma, as seen for PHR2, was not found in our study. Despite these differences, PHR1 colocalized with chromosomes in non-infected dividing cells in a similar manner to PHR2, suggesting that both PHR proteins are capable of binding condensed DNA.

ChchNPV PHR proteins also colocalized with mitotic spindle structures and midbodies, although the intensity of this fluorescence was low compared with the fluorescence of the chromosomes. From the primary function of DNA photolyases, namely repairing DNA lesions, interaction with DNA is crucial, but interactions with spindle structures consisting of microtubules cannot currently be explained. However, it is known that many proteins bind to the spindles; among these are also nucleic acid-binding proteins (Sauer *et al.*, 2005).

In this paper, we showed the nuclear localization of the two CPD photolyases encoded by ChchNPV in a transient insect cell expression system. The observed nuclear localization and DNA binding are prerequisites for a protein with a proposed function in the repair of baculovirus DNA. This is also the first report in which the interaction of CPD photolyases with chromosomes and spindle structures during mitosis has been visualized. The interaction of the viral PHRs with chromosomes and with virogenic stroma for PHR2 suggests that they can bind condensed DNA, a situation that exists in baculovirus nucleocapsids, both in incoming parental virions and in assembling progeny nucleocapsids (Rohrmann, 2008). Our next goal is to investigate whether baculovirus photolyases end up in baculovirus virions.

METHODS

Plasmids. The coding region of Cc-*phr1* was amplified by PCR with Phusion high-fidelity DNA polymerase (Finnzymes) using genomic DNA of the Dutch ChchNPV isolate (ChchNPV-NL) as template. A *Hin*dIII restriction site was introduced upstream of the ORF and the stop codon was replaced with a *Bam*HI restriction site (see Supplementary Table S1, available in JGV Online, for primer sequences). The amplicons were cloned into pGEM-T (Promega) and the sequence was verified. The *phr1* fragment was subcloned between the *Hin*dIII and *Bam*HI sites located downstream of the *Orgyia pseudotsugata* multiple NPV (OpMNPV) immediate early 2 (*ie2*) promoter and upstream of the EGFP reporter gene in the vector PIZ-EGFP-N3 to generate PIZ-phr1-EGFP (Fig. 1a). In a similar way, the coding region of the Cc-*phr2* gene flanked by *Eco*RI and *Bam*HI restriction sites was amplified and cloned into PIZ-EGFP-N3 between the corresponding restriction sites to give PIZ-phr2-EGFP (Fig. 1b). The pIZ-EGFP-N3 vector was made by Dr Marcel Westenberg (Laboratory of Virology, Wageningen University) by cloning the EGFP sequence of pEGFP-N3 (Clontech) as a *Hin*dIII–*Not*I fragment into the corresponding sites of PIZ-V5/His (Invitrogen). PIZ-EGFP-N3 was also used as a control (Fig. 1c). The complete ORF of Cc-*phr2* with stop codon and flanked by *Eco*RI sites was recloned from a *phr2*-containing pGEM-T Easy vector (van Oers *et al.*, 2008) into the *Eco*RI site of PIZ/HIS-V5 (Invitrogen), resulting in PIZ-phr2 (Fig. 1d). For clarity, none of these coding regions was fused to the His tag or the V5 epitope as originally present in the PIZ-V5/HIS plasmid (Fig. 1e).

Anti-Cc-PHR2 polyclonal antiserum. In order to produce rabbit polyclonal antiserum against Cc-PHR2, the corresponding *phr2* gene was overexpressed in a photolyase-deficient *E. coli* strain (KY29) (Akasaka & Yamamoto, 1991) used with kind permission of Dr Kazuo Yamamoto (Dept of Biomolecular Sciences, Tohoku University, Japan). The overexpression and purification methods have been described before (van Oers *et al.*, 2008). Purified Cc-PHR2 (490 μg in 1 ml PBS) was emulsified with 1 ml Freund's incomplete adjuvant (Sigma) and used to immunize two rabbits. These rabbits had been selected for low signal in the pre-immune serum on Western blots using lysates of ChchNPV-infected *T. ni* High Five cells and human cell extract. After three booster injections with the same amount of antigen, sera were collected and stored at −80 °C after adding 0.1 % sodium azide.

Cell transfection and infection. *Trichoplusia ni* High Five cells (Invitrogen) were maintained as monolayer cultures in Express Five serum-free medium (Invitrogen) supplemented with 10 % L-glutamine (Gentaur). For transfections, 10^5 *T. ni* High Five cells were seeded in 35 mm Petri dishes (Nunc) in Express Five serum-free medium with 10 % L-glutamine. After attachment of the cells, the medium was replaced with Grace's non-supplemented insect medium (Sigma), to which 10 % L-glutamine was added. After incubation at 27 °C for 24 h, cells were transfected with 4 μg plasmid DNA using 10 μl cellfectin reagent (Invitrogen). After incubation at 27 °C for 3 h, the transfection mixture was replaced with 2 ml Express Five serum-free medium with 10 % L-glutamine, penicillin (30 μg ml^{-1}) and streptomycin (75 μg ml^{-1}). At 24 h p.t., the cells were infected with AcMNPV (E2 strain; Smith & Summers, 1978) at an m.o.i. of 10 $TCID_{50}$ units per cell. Cells were incubated at 27 °C until further analysis.

Western blot analysis. Transfected cells were harvested at 24 h p.t. and the proteins were separated by 10 % SDS-PAGE and transferred to Immobilon-P membrane (Millipore) by semi-dry electrophoretic transfer. The membranes were blocked overnight in 5 % non-fat milk in PBS buffer with 0.1 % Tween 20. The membranes were incubated with rabbit anti-Cc-PHR2 antibodies, diluted 1 : 500 in PBS with 0.5 % fat-free milk and 0.1 % Tween 20, for 1 h at room temperature. After three washes with the same buffer, alkaline phosphatase-conjugated goat anti-rabbit immunoglobulin (Dako) diluted 1 : 2000 was used as secondary antibody for 1 h. After washing, blots were stained with NBT/BCIP (Roche) in AP buffer (0.1 M Tris/HCl, pH 9.5, 0.1 M NaCl, 5 mM $MgCl_2$).

Confocal laser scan microscopy. EGFP fluorescence in transfected cells and cells that were subsequently infected was examined with a Zeiss LSM510 confocal laser scanning microscope using an FITC filter. For immunofluorescence, cells were collected at 24 h p.t. and allowed to attach to 0.05 % poly-L-lysine-coated microscope slides. The cells were fixed in 96 % ethanol for 20 min at room temperature and washed with PBS. After blocking for 30 min with PBS containing 10 % BSA, the cells were incubated with rabbit anti-Cc-PHR2 antiserum, diluted 1 : 500 in PBS with 1 % BSA, for 1 h at room temperature. Cells were washed three times with PBS. Rhodamine-linked goat-anti-rabbit IgG secondary antibodies (Molecular Probes) (diluted 1 : 200, 1 h at 37 °C in the dark) were used to detect the primary antibodies. After washing, imaging was performed with a Zeiss LSM510 confocal laser scanning microscope using a rhodamine filter.

ACKNOWLEDGEMENTS

F. X. was supported by a PhD grant from the Royal Dutch Academy of Arts and Sciences (project 05Phd01). M. M. v. O. was supported by a MEERVOUD grant from the Research Council of Earth and Life Sciences (ALW) with financial aid from the Netherlands Organization for Scientific Research (NWO) (project 836.05.070). Monika Bajek is acknowledged for her help in antibody preparation.

REFERENCES

Akasaka, S. & Yamamoto, K. (1991). Construction of *Escherichia coli* K12 *phr* deletion and insertion mutants by gene replacement. *Mutat Res* **254**, 27–35.

Aubert, C., Vos, M. H., Mathis, P., Eker, A. P. M. & Brettel, K. (2000). Intraprotein radical transfer during photoactivation of DNA photolyase. *Nature* **405**, 586–590.

Chiganças, V., Batista, L. F. Z., Brumatti, G., Amarante-Mendes, G. P., Yasui, A. & Menck, C. F. M. (2002). Photorepair of RNA polymerase arrest and apoptosis after ultraviolet irradiation in normal and XPB deficient rodent cells. *Cell Death Differ* **9**, 1099–1107.

Deisenhofer, J. (2000). DNA photolyases and cryptochromes. *Mutat Res DNA Repair* **460**, 143–149.

Essen, L. O. & Klar, T. (2006). Light-driven DNA repair by photolyases. *Cell Mol Life Sci* **63**, 1266–1277.

Fritsch, E. & Huber, J. (1985). Inactivation of codling moth granulosis virus by UV-irradiation and temperature. *Nachr Dtsch Pflanzenschutzd* **37**, 84–88.

Hearst, J. E. (1995). The structure of photolyase: using photon energy for DNA repair. *Science* **268**, 1858–1859.

Ignoffo, C. M. & Garcia, C. (1992). Combinations of environmental factors and simulated sunlight affecting activity of inclusion bodies of the *Heliothis* (Lepidoptera: Noctuidae) nucleopolyhedrosis virus. *Environ Entomol* **21**, 210–213.

Jehle, J. A., Blissard, G. W., Bonning, B. C., Cory, J. S., Herniou, E. A., Rohrmann, G. F., Theilmann, D. A., Thiem, S. M. & Vlak, J. M. (2006). On the classification and nomenclature of baculoviruses: a proposal for revision. *Arch Virol* **151**, 1257–1266.

Kimura, S., Tahira, Y., Ishibashi, T., Mori, Y., Mori, T., Hashimoto, J. & Sakaguchi, K. (2004). DNA repair in higher plants; photoreactivation is the major DNA repair pathway in non-proliferating cells while excision repair (nucleotide excision repair and base excision repair) is active in proliferating cells. *Nucleic Acids Res* **32**, 2760–2767.

Ljungman, M. & Zhang, F. (1996). Blockage of RNA polymerase as a possible trigger for u.v. light-induced apoptosis. *Oncogene* **13**, 823–831.

Mitchell, D. L. & Nairn, R. S. (1989). The biology of the (6–4) photoproduct. *Photochem Photobiol* **49**, 805–819.

Nishigaki, R., Mitani, H. & Shima, A. (1998). Evasion of UVC-induced apoptosis by photorepair of cyclobutane pyrimidine dimers. *Exp Cell Res* **244**, 43–53.

Rohrmann, G. F. (2008). The baculovirus replication cycle: effects on cells and insects. In *Baculovirus Molecular Biology*. Bethesda, MD: National Library of Medicine/NCBI. http://www.ncbi.nlm.nih.gov/bookshelf/br.fcgi?book=bacvir&part=ch03

Rycyna, R. E. & Alderfer, J. L. (1985). UV irradiation of nucleic acids: formation, purification and solution conformational analysis of the '6–4 lesion' of dTpdT. *Nucleic Acids Res* **13**, 5949–5963.

Sancar, A. (1994). Structure and function of DNA photolyase. *Biochemistry* **33**, 2–9.

Sancar, A. (2003). Structure and function of DNA photolyase and cryptochrome blue-light photoreceptors. *Chem Rev* **103**, 2203–2237.

Sauer, G., Korner, R., Hanisch, A., Ries, A., Nigg, E. A. & Sillje, H. H. W. (2005). Proteome analysis of the human mitotic spindle. *Mol Cell Proteomics* **4**, 35–43.

Schul, W., Jans, J., Rijksen, Y. M. A., Klemann, K. H. M., Eker, A. P. M., de Wit, J., Nikaido, O., Nakajima, S., Yasui, A. & other authors (2002). Enhanced repair of cyclobutane pyrimidine dimers and improved UV resistance in photolyase transgenic mice. *EMBO J* **21**, 4719–4729.

Setlow, R. B. & Carrier, W. L. (1966). Pyrimidine dimers in ultraviolet-irradiated DNA's. *J Mol Biol* **17**, 237–254.

Smith, G. E. & Summers, M. D. (1978). Analysis of baculovirus genomes with restriction endonucleases. *Virology* **89**, 517–527.

Sun, X., Sun, X., Van Der Werf, W., Vlak, J. M. & Hu, Z. (2004). Field inactivation of wild-type and genetically modified *Helicoverpa armigera* single nucleocapsid nucleopolyhedrovirus in cotton. *Biocontrol Sci Technol* **14**, 185–192.

Vail, P. V., Hostetter, D. L. & Hoffmann, D. F. (1999). Development of the multi-nucleocapsid nucleopolyhedroviruses (MNPVs) infectious to loopers (Lepidoptera: Noctuidae: Plusiinae) as microbial control agents. *Integ Pest Manag Rev* **4**, 231–257.

van Oers, M. M., Herniou, E. A., Usmany, M., Messelink, G. J. & Vlak, J. M. (2004). Identification and characterization of a DNA photolyase-containing baculovirus from *Chrysodeixis chalcites*. *Virology* **330**, 460–470.

van Oers, M. M., Abma-Henkens, M. H. C., Herniou, E. A., de Groot, J. C. W., Peters, S. & Vlak, J. M. (2005). Genome sequence of *Chrysodeixis chalcites* nucleopolyhedrovirus, a baculovirus with two DNA photolyase genes. *J Gen Virol* **86**, 2069–2080.

van Oers, M. M., Lampen, M. H., Bajek, M. I., Vlak, J. M. & Eker, A. P. M. (2008). Active DNA photolyase encoded by a baculovirus from the insect *Chrysodeixis chalcites*. *DNA Repair (Amst)* **7**, 1309–1318.

Wang, Y., Choi, J. Y., Roh, J. Y., Woo, S. D., Jin, B. R. & Je, Y. H. (2008). Molecular and phylogenetic characterization of *Spodoptera litura* granulovirus. *J Microbiol* **46**, 704–708.

Williams, G. V. & Faulkner, P. (1997). Cytological changes and viral morphogenesis during baculovirus infection. In *The Baculoviruses*, pp. 61–108. Edited by L. K. Miller. New York: Plenum Press.

Willis, L. G., Siepp, R., Stewart, T. M., Erlandson, M. A. & Theilmann, D. A. (2005). Sequence analysis of the complete genome of *Trichoplusia ni* single nucleopolyhedrovirus and the identification of a baculoviral photolyase gene. *Virology* **338**, 209–226.

Xu, F., Vlak, J. M. & van Oers, M. M. (2008). Conservation of DNA photolyase genes in group II nucleopolyhedroviruses infecting plusiine insects. *Virus Res* **136**, 58–64.

Yasui, A., Eker, A. P. M., Yasuhira, S., Yajima, H., Kobayashi, T., Takao, M. & Oikawa, A. (1994). A new class of DNA photolyases present in various organisms including aplacental mammals. *EMBO J* **13**, 6143–6151.